

Sampled-Data Controllers for Autonomous Vehicles on Lane-Free Roads

Dionysis Theodosis, Filippos N. Tzortzoglou, Iasson Karafyllis,
Ioannis Papamichail and Markos Papageorgiou, *Life Fellow, IEEE*

Abstract—In this paper, we design decentralized control strategies (per vehicle) for the two-dimensional movement of autonomous vehicles on lane-free roads, where each vehicle determines its control input based on its own state and the relative speeds and distances from adjacent vehicles and from the boundaries of the road. It is shown that the vehicles do not collide with each other or with the road boundaries, and all vehicle speeds converge to a given longitudinal speed set-point. Moreover, we present sufficient conditions for the emulated (sampled-data) controllers that ensure collision avoidance between vehicles and with the road boundaries, as well as speed positivity, bounded speed and bounded orientation of the vehicles. Finally, we numerically investigate the maximum allowable sampling period and present periodic and non-periodic sampling algorithms where each vehicle has its own sampling period.

I. INTRODUCTION

Vehicle automation has made tremendous advances in the last decades and addresses different kinds of driver support systems ranging from Adaptive Cruise Control (ACC) and lane-assist systems to Cooperative ACC (CACC) and fully autonomous driving (see [2], [4], [10], [14], [18], [19]).

Recently, launched by [13], new principles were proposed for autonomous vehicles operating on lane-free roads ([9], [11], [16], [20]) that may improve traffic flow and increase capacity of highways. The vehicles do not abide to a lane discipline, as in conventional traffic, and can move on the two-dimensional surface of the lane-free road. In addition to lane-free traffic, another associated concept that can improve the flow of vehicles on a road is the concept of ‘nudging’ [13]. Nudging implies a virtual force that vehicles apply to the vehicles in front of them, and it has been shown that nudging can increase the flow in a ring-road and can have a strong stabilizing effect; see [6] and references therein.

Some microscopic models have been recently proposed, attempting to describe vehicle movement with low lane discipline by their human drivers; see [1], [5], [12]. The performance of such models, however, is naturally limited

The research leading to these results has received funding from the European Research Council under the European Union’s Horizon 2020 Research and Innovation programme ERC Grant Agreement n. [833915], project TrafficFluid.

D. Theodosis, F. N. Tzortzoglou, I. Papamichail, and M. Papageorgiou are with the Dynamic Systems and Simulation Laboratory, Technical University of Crete, Chania 73100, Greece. M. Papageorgiou is also with the Faculty of Maritime and Transportation, Ningbo University, Ningbo, China. dtheodosis@dssl.tuc.gr, ftzortzoglou@isc.tuc.gr, ipapa@dssl.tuc.gr, markos@dssl.tuc.gr

I. Karafyllis is with the Dept. of Mathematics, National Technical University of Athens, Zografou Campus 15780 Athens, Greece iasonkar@central.ntua.gr

by the limited perception and decision capabilities of human drivers, which are strongly inferior to the potential capabilities of autonomous vehicles.

In this paper, we consider identical autonomous vehicles described by the bicycle kinematic model. The bicycle kinematic model is selected because of its ability to capture non-holonomic constraints of the actual vehicle (see [14]). We design a family of novel nonlinear decentralized controllers for the safe operation of the vehicles on lane-free roads with the following features, which hold globally (Theorem 1): (i) the vehicles do not collide with each other or with the boundary of the road; (ii) the speeds of all vehicles are always positive and remain below a given speed limit; (iii) all vehicle speeds converge to a given longitudinal speed set-point; and (iv) the accelerations, lateral speeds, angular speeds and orientations of all vehicles tend to zero.

Moreover, we investigate the sample-and-hold implementation of the derived continuous-time controllers and present sufficient conditions for the emulated (sampled-data) controllers that ensure collision avoidance between vehicles and with the road boundaries, as well as speed positivity, bounded speed and bounded orientation of the vehicles (Lemma 1 and Lemma 2). Finally, we demonstrate that the proposed sufficient conditions can also be used for non-periodic sampling of the controllers where each vehicle has its own sampling period.

The structure of the paper is as follows. Section II is devoted to the presentation of the continuous-time controller and its properties. Section III contains the sampled-data model and certain sufficient conditions for the sample-and-hold implementation of the controllers; and in Section IV we numerically investigate the maximum allowable sampling period with the emulated controllers. In Section V, we present numerical examples to demonstrate the efficiency of the proposed decentralized cruise controllers under periodic and (state-dependent) non-periodic sampling. Finally, some concluding remarks are given in Section VI.

Notation. Throughout this paper, we adopt the following notation. $\mathbb{R}_+ := [0, +\infty)$ denotes the set of non-negative real numbers. By $|x|$ we denote both the Euclidean norm of a vector $x \in \mathbb{R}^n$ and the absolute value of a scalar $x \in \mathbb{R}$. By $|x|_\infty = \max\{|x_i|, i = 1, \dots, n\}$ we denote the infinity norm of a vector $x = (x_1, x_2, \dots, x_n)' \in \mathbb{R}^n$. Let $A \subseteq \mathbb{R}^n$ be an open set. By $C^0(A, \Omega)$, we denote the class of continuous functions on $A \subseteq \mathbb{R}^n$, which take values in $\Omega \subseteq \mathbb{R}^m$. By $C^k(A; \Omega)$, where $k \geq 1$ is an integer, we denote the class of functions on $A \subseteq \mathbb{R}^n$ with continuous derivatives of order k , which take values in $\Omega \subseteq \mathbb{R}^m$.

II. CONTINUOUS-TIME MODEL

Consider n vehicles on a lane-free road of width $2a > 0$, where the movement of each vehicle is described by the bicycle kinematic model

$$\begin{aligned}\dot{x}_i &= v_i \cos(\theta_i) \\ \dot{y}_i &= v_i \sin(\theta_i) \\ \dot{\theta}_i &= \sigma^{-1} v_i \tan(\delta_i) \\ \dot{v}_i &= F_i\end{aligned}\quad (1)$$

for $i = 1, \dots, n$, where $\sigma > 0$ is the length of each vehicle, (a constant). Here, $(x_i, y_i) \in \mathbb{R} \times (-a, a)$ is the reference point of the i -th vehicle in an inertial frame with Cartesian coordinates (X, Y) , with $i \in \{1, \dots, n\}$ and is placed at the midpoint of the rear axle of the vehicle, $v_i \in (0, v_{\max})$ is the speed of the i -th vehicle, where $v_{\max} > 0$ denotes the road speed limit, $\theta_i \in (-\frac{\pi}{2}, \frac{\pi}{2})$ is the orientation of the i -th vehicle with respect to the X axis, δ_i is the steering angle of the front wheels relative to the orientation θ_i of the i -th vehicle, and F_i is the acceleration of the i -th vehicle. $F_i, \delta_i \in \mathbb{R}$ are the control inputs of the model. Let $v^* \in (0, v_{\max})$ be given (the speed set-point) and define the set

$$S := \mathbb{R}^n \times (-a, a)^n \times (-\varphi, \varphi)^n \times (0, v_{\max})^n \quad (2)$$

where $\varphi \in (0, \frac{\pi}{2})$ is an angle that satisfies

$$\cos(\varphi) > \frac{v^*}{v_{\max}} \quad (3)$$

The set S in (2) describes all possible states of the system of n vehicles. More specifically, each vehicle should stay within the road, i.e., $(x_i, y_i) \in \mathbb{R} \times (-a, a)$ for $i = 1, \dots, n$, the vehicles should not be able to turn perpendicular to the road, i.e., $\theta_i \in (-\varphi, \varphi)$, $i = 1, \dots, n$, and the speeds of all vehicles should always be positive, i.e., no vehicle moves backwards; and respect the road speed limits. The constant φ is a safety constraint, to restrict the movement of a vehicle.

In what follows, we assume that the distance between vehicles is defined by

$$d_{i,j} := \sqrt{(x_i - x_j)^2 + p(y_i - y_j)^2} \text{ for } i, j = 1, \dots, n \quad (4)$$

where $p > 0$ is a weighting factor. Note that for $p = 1$ we obtain the standard Euclidean distance, while for larger values of $p > 1$, we have an ‘‘elliptical’’ metric which will allow to approximate more accurately the dimensions of a vehicle. The optimal selection of p can be found in [7].

Let

$$w = (x_1, \dots, x_n, y_1, \dots, y_n, \theta_1, \dots, \theta_n, v_1, \dots, v_n)' \in \mathbb{R}^{4n} \quad (5)$$

Due to the various constraints that were explained above, the state space of the model (1) is

$$\Omega := \{w \in S : d_{i,j} > L, i, j = 1, \dots, n, j \neq i\} \quad (6)$$

where L is a given positive constant (the minimum inter-vehicle distance). Notice that the state space Ω is not a linear subspace of \mathbb{R}^{4n} , but an open set.

Let $V : (L, +\infty) \rightarrow \mathbb{R}_+$ and $U : (-a, a) \rightarrow \mathbb{R}_+$ be a C^2 functions that satisfy the following properties

$$\lim_{d \rightarrow L^+} (V(d)) = +\infty \quad (7)$$

$$V(d) = 0, \text{ for all } d \geq \lambda \quad (8)$$

$$\lim_{y \rightarrow (-a)^+} (U(y)) = +\infty, \lim_{y \rightarrow a^-} (U(y)) = +\infty \quad (9)$$

$$U(0) = 0 \quad (10)$$

$$\kappa(d) = 0, \text{ for all } d \geq \lambda \quad (11)$$

where $\lambda > L$ is a constant. The functions V and U above are potential functions, which have been widely used to avoid collisions between vehicles and the boundary of the road (see for instance [4], [15], [17], [19]). The function κ will be used in the subsequent analysis to characterize the derived controllers in terms of relative speeds from adjacent vehicles.

We apply, next, a control Lyapunov function methodology to design decentralized feedback laws that ensure the following properties:

- (P1) For $w(0) \in \Omega$, then $w(t) \in \Omega$ for all $t \geq 0$, which according to (6) implies that there are no collisions between vehicles ($d_{i,j}(t) > L$ for $t \geq 0$, $i, j = 1, \dots, n$, $j \neq i$) or with the boundary of the road ($y_i(t) \in (-a, a)$ for $t \geq 0$); the speeds of all vehicles are always positive and remain below the given speed limit, ($v_i(t) \in (0, v_{\max})$ for all $t \geq 0$); and the orientation of each vehicle is always bounded by the given value $\varphi \in (0, \frac{\pi}{2})$, ($\theta_i(t) \in (-\varphi, \varphi)$ for $t \geq 0$).
- (P2) The orientation of each vehicle satisfies $\lim_{t \rightarrow +\infty} \theta_i(t) = 0$, $i = 1, \dots, n$, and the speed of all vehicles satisfy $\lim_{t \rightarrow +\infty} v_i(t) = v^*$, $i = 1, \dots, n$, for a given a longitudinal speed set-point $v^* \in (0, v_{\max})$.
- (P3) The accelerations, angular speeds, and lateral speeds of all vehicles tend to zero, i.e., $\lim_{t \rightarrow +\infty} F_i(t) = 0$, $\lim_{t \rightarrow +\infty} \dot{\theta}_i(t) = 0$, and $\lim_{t \rightarrow +\infty} \dot{y}_i(t) = 0$, $i = 1, \dots, n$.

We define the Control Lyapunov Function, for all $w \in \Omega$,

$$\begin{aligned}H(w) &:= \frac{1}{2} \sum_{i=1}^n (v_i \cos(\theta_i) - v^*)^2 + \frac{1}{2} \sum_{i=1}^n v_i^2 \sin^2(\theta_i) \\ &+ \sum_{i=1}^n U(y_i) + \frac{1}{2} \sum_{i=1}^n \sum_{i \neq j} V(d_{i,j}) \\ &+ A \sum_{i=1}^n \left(\frac{1}{\cos(\theta_i) - \cos(\varphi)} - \frac{1}{1 - \cos \varphi} \right)\end{aligned}\quad (12)$$

where $A > 0$, $\beta > 1$ are parameters of the controller and the Lyapunov function, $v^* \in (0, v_{\max})$ is the given longitudinal speed set-point, and $\varphi \in (0, \frac{\pi}{2})$ is a constant that satisfies the inequality (3). This Lyapunov function is based on the mechanical energy of the system plus a penalty term to restrict the orientation of the vehicles, see [7] for details.

In what follows, we use the input transformation $\delta_i := \arctan(v_i^{-1} \sigma u_i)$ in (1), to obtain the following system

$$\dot{x}_i = v_i \cos(\theta_i), \dot{y}_i = v_i \sin(\theta_i), \dot{\theta}_i = u_i, \dot{v}_i = F_i \quad (13)$$

for $i = 1, \dots, n$, where u_i and F_i , are the inputs of the system.

The feedback laws for each vehicle $i = 1, \dots, n$ can be designed using (12), and the potential functions V and U that satisfy (7), (8) and (9), (10), respectively, as well as the function κ in (11):

$$u_i = \left(G_i(w) - U'(y_i) - p \sum_{j \neq i} V'(d_{i,j}) \frac{(y_i - y_j)}{d_{i,j}} - \sin(\theta_i) F_i \right) \times \left(v^* + \frac{A}{v_i (\cos(\theta_i) - \cos(\varphi))^2} \right)^{-1} \quad (14)$$

$$F_i = -\frac{1}{\cos(\theta_i)} (k_i(w) (v_i \cos(\theta_i) - v^*) + \Lambda_i(w)) \quad (15)$$

where

$$G_i(w) = -\mu_1 v_i \sin(\theta_i) + \sum_{j \neq i} \kappa(d_{i,j}) (v_j \sin(\theta_j) - v_i \sin(\theta_i)) \quad (16)$$

$$\Lambda_i(w) = \sum_{j \neq i} V'(d_{i,j}) \frac{(x_i - x_j)}{d_{i,j}} - \sum_{j \neq i} \kappa(d_{i,j}) (v_j \cos(\theta_j) - v_i \cos(\theta_i)) \quad (17)$$

and

$$k_i(w) = \mu_2 + \frac{\Lambda_i(w)}{v^*} + \frac{v_{\max} \cos(\theta_i)}{v^* (v_{\max} \cos(\theta_i) - v^*)} f(-\Lambda_i(w)) \quad (18)$$

and $f \in C^1(\mathbb{R})$ is any function that satisfies

$$\max(0, x) \leq f(x) \text{ for all } x \in \mathbb{R} \quad (19)$$

The term $k_i(w)$ in the acceleration $F_i(t)$ given by (15), is a state-dependent controller gain which guarantees that the speed of each vehicle will remain positive and less than the speed limit. The first term that appears on the right-hand side of (17), is the summation of repulsive forces ($V'(d)$) from vehicles that are in close proximity to vehicle i , and the summation of relative longitudinal speeds from vehicles that are in close proximity to vehicle i . If V in (14), (15) is decreasing, then, the second term of (14) is positive if vehicle j is behind vehicle i , i.e., $(x_i - x_j) > 0$. Indeed, in this case, we have that $-V'(d_{i,j})(x_i - x_j)d_{i,j}^{-1} > 0$, and this term represents the effect of nudging, since vehicles that are close and behind vehicle i will also exert a ‘‘pushing’’ force towards it that will increase its acceleration.

The following theorem addresses all properties (P1), (P2), and (P3).

Theorem 1: *For every $w_0 \in \Omega$ there exists a unique solution $w(t) \in \Omega$ of the initial-value problem (13), (14), (15) with initial condition $w(0) = w_0$. The solution $w(t) \in \Omega$ is defined for all $t \geq 0$ and satisfies for $i = 1, \dots, n$*

$$\lim_{t \rightarrow +\infty} (v_i(t)) = v^*, \lim_{t \rightarrow +\infty} (\theta_i(t)) = 0 \quad (20)$$

$$\lim_{t \rightarrow +\infty} (u_i(t)) = 0, \lim_{t \rightarrow +\infty} (F_i(t)) = 0 \quad (21)$$

Moreover, there exist non-decreasing functions $Q_k : \mathbb{R}_+ \rightarrow \mathbb{R}_+$ ($k = 1, 2$) such that $|F_i(t)| \leq Q_1(H(w(0)))$, $|u_i(t)| \leq Q_2(H(w(0)))$, for all $t \geq 0$, $i = 1, \dots, n$ and for every solution $w(t) \in \Omega$ of (13), (14), (15).

Remarks: (i) Properties (7) and (11) guarantee that the feedback laws (14), (15) depend only on information from adjacent vehicles, namely from vehicles that are located at a distance less than $\lambda > 0$.

(ii) Compared to [7], the feedback laws (14), (15) also depend on the lateral relative speed, and longitudinal relative speed from vehicles in the vicinity of vehicle i , (see (16) and (17), respectively). This modification of the controllers gives a smoother convergence to the speed set-point v^* .

(iii) Due to space constraints the proof of Theorem 1 is omitted. The reader is referred to [8] for the proofs of a general result that includes the results of Theorem 1 and also the case of vehicles of different lengths.

III. SAMPLED-DATA MODEL

For the actual implementation of the controllers, a typical approach is that of emulation: a continuous-time controller is designed initially to satisfy certain closed-loop control specifications; and then it is implemented as a digital controller. More specifically, the control inputs F_i , δ_i are digitalized and produce a sequence of control values $F_i(t_k)$, $\delta_i(t_k)$ using the sampled version of the system’s state $w(t_k)$ at each sampling instant $t_{k+1} = t_k + T$, $k = 0, 1, 2, \dots$, $T > 0$, t_0 being the initial time, (see [3] and references therein).

We consider next the emulation of the controllers (14), (15). For brevity and conciseness, let

$$\omega_i := \sigma^{-1} \tan(\delta_i), \text{ for } i = 1, \dots, n. \quad (22)$$

where $\delta_i := \arctan(v_i^{-1} \sigma u_i)$. Assuming therefore, that F_i, ω_i are constant on the time interval $[t, t + T)$, $T > 0$, $t \geq 0$, we obtain with direct integration from (1), the following exact discrete bicycle model:

If $\omega_i \neq 0$

$$\begin{aligned} x_i(t+s) &= x_i(t) \\ &+ \frac{1}{\omega_i} \left(\sin \left(\theta_i(t) + \omega_i \left(v_i(t) + \frac{1}{2} s F_i \right) s \right) - \sin(\theta_i(t)) \right) \\ y_i(t+s) &= y_i(t) \\ &+ \frac{1}{\omega_i} \left(\cos(\theta_i(t)) - \cos \left(\theta_i(t) + \omega_i \left(v_i(t) + \frac{1}{2} s F_i \right) s \right) \right) \\ \theta_i(t+s) &= \theta_i(t) + \left(v_i(t) + \frac{1}{2} s F_i \right) s \omega_i \\ v_i(t+s) &= v_i(t) + s F_i \end{aligned} \quad (23)$$

for all $s \in [0, T]$; and if $\omega_i = 0$

$$\begin{aligned} x_i(t+s) &= x_i(t) + v_i(t) \cos(\theta_i(t)) s + F_i \cos(\theta_i(t)) \frac{s^2}{2} \\ y_i(t+s) &= y_i(t) + v_i(t) \sin(\theta_i(t)) s + F_i \sin(\theta_i(t)) \frac{s^2}{2} \\ \theta_i(t+s) &= \theta_i(t) \\ v_i(t+s) &= v_i(t) + s F_i \end{aligned} \quad (24)$$

for all $s \in [0, T]$.

The following lemma gives certain sufficient conditions for the sampling period T in order for a vehicle i to avoid collisions with other adjacent vehicles and the road

boundaries, and to have bounded orientation and bounded speed within speed limits.

Lemma 1: Let $T > 0$ and consider model (23), (24) with $F_i(t) \equiv F_i, \omega_i(t) \equiv \omega_i$ for all $t \in [0, T]$, $k = 1, \dots, n$. Let $w(0) \in \Omega$ be given, where Ω is defined by means of (6). Let also an arbitrary index $i \in \{1, \dots, n\}$ be given and suppose that for each $j = 1, \dots, n$, $j \neq i$ it holds that $v_j(T) \in (0, v_{\max})$ and $\theta_j(T) \in (-\varphi, \varphi)$. Moreover, assume that the following inequalities hold

$$T < \min \left\{ \frac{a - |y_i(0)|}{v_{\max} \sin(\varphi)}, \frac{\min_{j \neq i} \{d_{i,j}(0) - L\}}{\delta} \right\} \quad (25)$$

$$-\frac{v_i(0)}{T} < F_i(0) < \frac{v_{\max} - v_i(0)}{T} \quad (26)$$

$$\frac{-\varphi - \theta_i(0)}{v_i(0)T + \frac{1}{2}F_i T^2} < \omega_i(0) < \frac{\varphi - \theta_i(0)}{v_i(0)T + \frac{1}{2}F_i T^2} \quad (27)$$

where $\delta = \sqrt{2}v_{\max}\sqrt{1 + (2p-1)\sin^2(\varphi)}$. Then, $v_i(t) \in (0, v_{\max})$, $\theta_i(t) \in (-\varphi, \varphi)$, $y_i(t) \in (-a, a)$, and $d_{i,j}(t) > L$, for all $t \in [0, T]$, $j = 1, \dots, n$, $j \neq i$.

Lemma 1 provides an upper bound on the sampling period for a vehicle i to satisfy property (P1). In practice, each vehicle has its own internal clock and may also have its own sampling period, even in the case of identical vehicles. Lemma 1, can therefore be exploited to select the sampling period for each vehicle based on the distance of other vehicles and the road boundaries, see Section V.

Lemma 2: Let $w(0) \in \Omega$ be given, where Ω is defined by means of (6) and consider model (23), (24) with $F_i(t) \equiv F_i$, $\omega_i(t) \equiv \omega_i \in \mathbb{R}$, $i = 1, \dots, n$ being constant for all $t \in [0, T]$. Suppose also that (25), (26) and (27) hold for all $i = 1, \dots, n$. Then $w(t) \in \Omega$ for all $t \in [0, T]$.

Lemma 2 suggests that if T is the same for all vehicles and satisfies (25), (26) and (27) for all $i = 1, \dots, n$, then the following implication holds: $w(0) \in \Omega \Rightarrow w(t) \in \Omega$ for all $t \in [0, T]$. Lemma 2 can also be exploited for non-periodic sampling with all vehicles having the same period T . Due to space constraints the proofs of the above lemmas are omitted.

IV. NUMERICAL INVESTIGATION OF MAXIMUM ALLOWABLE SAMPLING PERIOD

In this section, we examine the Maximum Allowable Sampling Period (MASP) for the sampled-data system (23) with the controller (14), (15). Namely, we investigate the maximum $T > 0$ for which $w(t) \in \Omega$, $t \geq 0$ for all $w(0) \in \Omega$. Let

$$V(d) = \begin{cases} q_1 \frac{(\lambda-d)^3}{d-L} & , L < d \leq \lambda \\ 0 & , d > \lambda \end{cases} \quad (28)$$

$$U(y) = \begin{cases} \left(\frac{1}{a^2-y^2} - \frac{c}{a^2} \right)^4 & , -a < y < -\frac{a\sqrt{c-1}}{\sqrt{c}} \\ \text{and } \frac{a\sqrt{c-1}}{\sqrt{c}} < y < a \\ 0 & -\frac{a\sqrt{c-1}}{\sqrt{c}} \leq y \leq \frac{a\sqrt{c-1}}{\sqrt{c}} \end{cases} \quad (29)$$

$$\kappa(d) = \begin{cases} q_2(\lambda-d)^2 & , L < d \leq \lambda \\ 0 & , d > \lambda \end{cases} \quad (30)$$

$$f(x) = \frac{1}{2\varepsilon} \begin{cases} 0 & \text{if } x \leq -\varepsilon \\ (x+\varepsilon)^2 & \text{if } -\varepsilon < x < 0 \\ \varepsilon^2 + 2\varepsilon x & \text{if } x \geq 0 \end{cases} \quad (31)$$

where $0 < L < \lambda$, $\varepsilon > 0$, $c > 1$ and $q_1 > 0$, $q_2 \geq 0$.

To study numerically the MASP of the model, we consider initial conditions $w(0) \in \Omega$ which satisfy $H(w(0)) = \ell \in \mathbb{R}_+$ for certain values of $\ell > 0$, where H is defined in (12). Finally, we will consider both the case where the vehicles only measure the distance from neighboring vehicles ($q_2 = 0$ in (30)) and the case where the vehicles can also use the relative speeds of adjacent vehicles ($q_2 \neq 0$ in (30)).

Fig. 1 shows the MASP for both cases $q_2 = 0$ and $q_2 \neq 0$ for increasing values of $H(w(0))$. With blue is the MASP when $q_2 = 0$, with red is the MASP when $q_2 = 0.03$, and with yellow the MASP when $q_2 = 0.1$. It can be seen that, as the value of H increases, the MASP decreases, while the MASP is larger for higher values of q_2 .

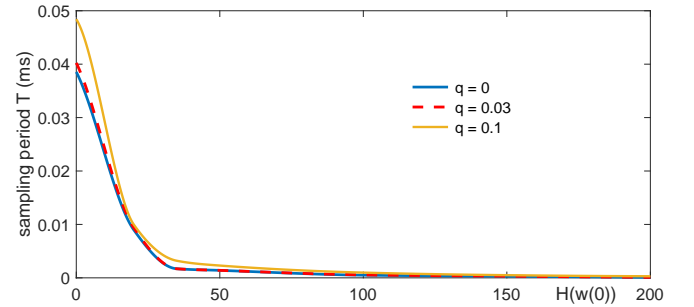


Fig. 1: The sampling times T for increasing values of H , for the system (23) with (14), (15).

For the previous results, we have used $n = 10$, $\sigma = 5m$, $v_{\max} = 35m/s$, $a = 7.2m$, $v^* = 30m/s$, $\varphi = 0.25$ (in order to satisfy condition (2.3)), $p = 5.11$, $L = 5.59m$, $\varepsilon = 0.2$, $\mu_1 = 0.5$, $\mu_2 = 0.1$, $q_1 = 3 \cdot 10^{-3}$, $\lambda = 25m$, $A = 1$ and $c = 1.5$. The selection of those values was based on [7], which also includes a general description on the selection of appropriate gains. It should be noted that the approximation of the MASP above, corresponds to the specific selection of the potential functions V , U and the various constants associated with them. For a different selection, it is possible to obtain higher values for the MASP.

V. SIMULATIONS

In the following simulation scenarios, we consider the use of periodic, non-periodic and state-dependent sampling periods T . We will consider both the cases $\kappa(d)$ satisfying (11), and the case $\kappa(d) \equiv 0$, by selecting q_2 in (30) appropriately. Our standing assumption is that for all vehicles the initial sampling time is at $t = 0$.

We consider $n = 10$ vehicles on a lane-free road modeled by (1) with the feedback laws (14), (15), and f given by means of (31). The vehicle-repulsive potential function V and the boundary-repulsive potential function U are defined in (28), (29), respectively. In all simulation scenarios below, we consider the same initial conditions and we use the same parameters and controller gains as in Section IV.

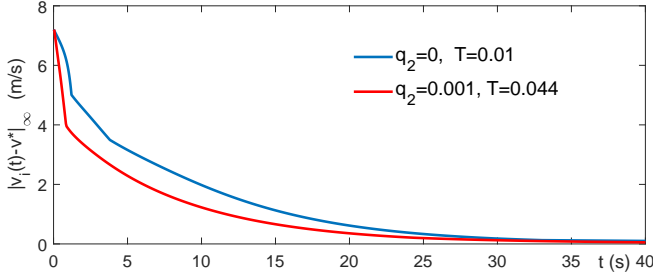


Fig. 2: Convergence of $|v_i(t) - v^*|_\infty$ for $q_2 = 0$ with blue and $q_2 = 0.001$ with red.

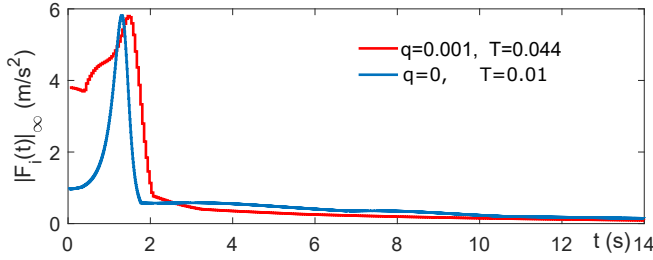


Fig. 3: Maximum acceleration $|F_i(t_k)|_\infty$ for $q_2=0$ and $q_2 \neq 0$.

Scenario 1: In this scenario, we consider a constant sampling period $T > 0$ (the same for all vehicles) that is selected to satisfy the conditions of Lemma 2. It is observed that, for $q_2 = 0$ and $T = 0.01$, no collisions occur, whereas in the case of $T = 0.02$ there are collisions with the boundary of the road. When $q_2 = 0.001$ and $T = 0.044$, no collisions occur, whereas in the case of $T = 0.047$ there are collisions. Note that for the specific initial conditions of this scenario, the values of T above, are much larger than the MASP, which for this case ($H(w(0)) = 96$), is $T_{MASP} = 5 \cdot 10^{-3}$ (recall that the MASP is approximated by over all $w_0 \in \Omega$). Fig. 2 shows the convergence of the speed to the speed set-point v^* for $q_2 = 0$ (blue) and $q_2 \neq 0$ (red). It can be seen that the speed converges faster to v^* when $q_2 \neq 0$. Fig. 3 shows the accelerations $|F_i(t_k)|_\infty$. For $q_2 \neq 0$ we have higher initial acceleration which contributes to the faster convergence of the speed to the longitudinal speed set-point.

Scenario 2: In this scenario, the sampling period T (same for all vehicles) is not constant, but is dynamically calculated on the basis of Lemma 2. In particular, T is calculated according to the formula

$$T_k = \max \left\{ \alpha, \beta \min_{i=1, \dots, n} \left\{ \frac{a - |y_i(t_k)|}{v_{\max} \sin(\varphi)}, \frac{\min_{j \neq i} \{d_{i,j}(t_k) - L\}}{\delta} \right\} \right\}$$

where $t_{k+1} = t_k + T_k$, $k = 0, 1, \dots$, $\alpha > 0$, $\beta \in (0, 1)$. The constant $\alpha > 0$ provides a lower bound on the sampling period, and β adjusts the sampling period in order for (25) to hold. We set $\alpha = 10^{-4}$ and $\beta = 0.9$. Fig. 4 shows the non-periodic sampling instants for both cases of $q_2 = 0$ and $q_2 \neq 0$ compared to the periodic sampling of Scenario 1. When $q_2 \neq 0$, the sampling period T becomes larger when the vehicles' speed approaches the set-point v^* and approaches a constant value depending on the minimum inter-vehicle distance and the minimum distance from the road boundaries for all 10 vehicles. Finally, it can be seen

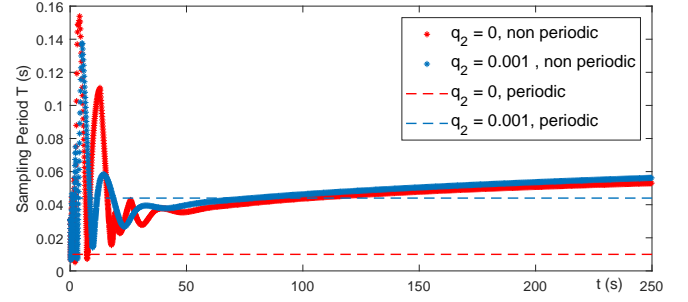


Fig. 4: The aperiodic sampling instants for $q_2 = 0$ and $q_2 \neq 0$ compared to the periodic sampling of Scenario 1.

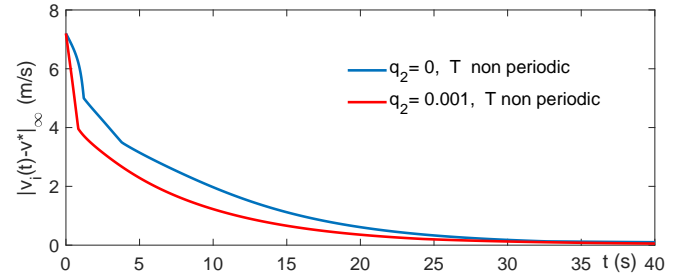


Fig. 5: Convergence of $|v_i(t) - v^*|_\infty$ for $q_2 = 0$ and $q_2 = 0.001$ in Scenario 2.

from Fig. 5, that, when $q_2 \neq 0$, the vehicle speeds converge faster to their desired speed. For the time-interval $[0, 300s]$, the simulation's runtime was $47s$ for $q_2 = 0$ and $41s$ for $q_2 \neq 0$, on a machine powered by Intel Core $i5 - 6200$, 2.30 Ghz, with Matlab. For Scenario 1, the simulation's runtime was $204s$ for $q_2 = 0$ and $80s$ for $q_2 \neq 0$,

Note that the computation of T_k calls for data from all vehicles, hence this handling of sample time may be valuable to speed up the simulation, but it is not for use by real vehicles. In Scenario 3 below, we consider state-dependent sample times, which are different for each vehicle and can be computed based on decentralized data.

Scenario 3: In this particular simulation scenario, we consider the case where each vehicle has its own sampling period T_i that changes dynamically at each sampling instant t_k^i , $k = 0, 1, \dots$ (t_k^i denotes the sampling time of vehicle i). We assume that at each sampling time t_k^i , vehicle i can measure through sensors, the relative speeds and distances from adjacent vehicles and the distance from the boundary of the road. Each vehicle's sampling period T_i is calculated on the basis of Lemma 1, according to the formula

$$T_k^i = \max \left\{ \alpha, \beta \min \left\{ \frac{a - |y_i(t_k^i)|}{v_{\max} \sin(\varphi)}, \frac{\min_{j \neq i} \{d_{i,j}(t_k^i) - L_j\}}{\delta} \right\} \right\}$$

where $t_{k+1}^i = t_k^i + T_k^i$, $k = 0, 1, \dots$, $\alpha > 0$, $\beta \in (0, 1)$, provided that constraints (26) and (27) hold. Fig. 6 and Fig. 7 show the (state-dependent) sampling periods of 4 of the vehicles for $q_2=0$ and $q_2=0.001$, respectively. It can be seen that all vehicles have different sampling periods which is adjusted based on their distance from other adjacent vehicles

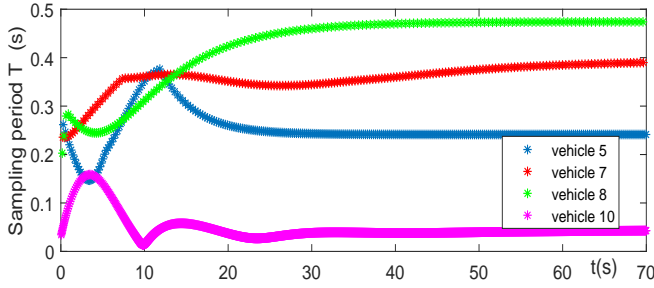


Fig. 6: The sampling periods of 4 of the vehicles during the episode for $q_2 = 0$.

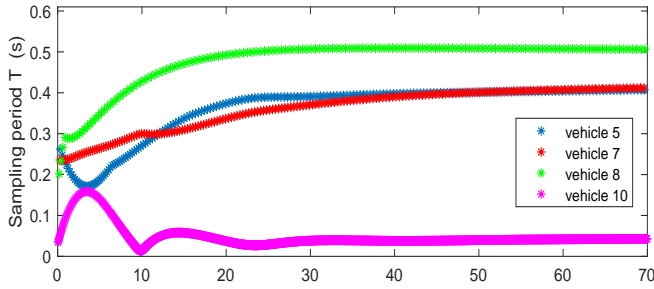


Fig. 7: The sampling periods of 4 of the vehicles during the episode for $q_2 = 0.001$.

and the boundary of the road. Also, it should be noted that, when $q_2 = 0$ the average T is smaller. More specifically, the average T across all vehicles for 300s of simulation time, when $q_2 = 0$, is $T_{avg} = 0.149$, and for the case of $q_2 \neq 0$, we have $T_{avg} = 0.159$. Notice that in Scenario 2, we have that $T_{avg} = 0.051$ and $T_{avg} = 0.054$ for $q_2 = 0$ and $q_2 \neq 0$, respectively, which are almost equal to T_{avg} of vehicle 10 in Fig. 6 and Fig. 7 of Scenario 3. Fig. 8 presents the minimum inter-vehicle distance between all vehicles establishing that there are no collisions among vehicles.

VI. CONCLUSION

We have presented decentralized (per vehicle) controllers for autonomous vehicles operating on lane-free roads that guarantee that there are no collisions among vehicles and with the road boundaries, and all vehicles attain a desired speed. Moreover, we have investigated the sample-and-hold implementation of the continuous-time controllers and we have demonstrated the use of non-periodic sampling where each vehicle has its own sampling period. In future work, we will study the qualitative properties of the emulated controller, (stability, convergence etc.) with both periodic and non-periodic sampling. The difficulty of this subject stems from the facts that the closed-loop system evolves on an open set (a case not studied in the literature where the state space is usually the space \mathbb{R}^n) and the function H is not a strict Lyapunov function; and therefore standard techniques from sampled-data feedback and self-triggered control are not directly applicable.

REFERENCES

[1] G. Asaithambi, V. Kanagaraj, and T. Toledo, "Driving Behaviors: Models and Challenges for Non-Lane Based Mixed Traffic", *Transportation in Developing Economies*, 2, 2016.

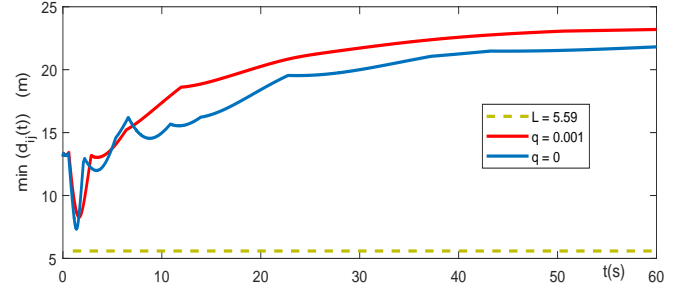


Fig. 8: The minimum inter-vehicle distance.

- [2] J. Guanetti, Y. Kim, F. Borrelli, "Control of connected and automated vehicles: State of the art and future challenges", *Annual Reviews in Control*, 45, 2018, 18-40.
- [3] L. Hetel, C. Fiter, H. Omran, A. Seuret, E. Fridman, J.-P. Richard, S. I. Niculescu, "Recent developments on the stability of systems with aperiodic sampling: An overview", *Automatica*, 76, 2017, 309-335.
- [4] L. Iftekhar and R. Olfati-Saber, "Autonomous Driving for Vehicular Networks with Nonlinear Dynamics," *2012 IEEE Intelligent Vehicles Symposium*, 2012, 723-729.
- [5] V. Kanagaraj, M. Treiber, "Self-driven Particle Model for Mixed Traffic and Other Disordered Flows", *Physica A: Statistical Mechanics and its Applications*, 509, 2018, 1-11.
- [6] I. Karafyllis, D. Theodosis and M. Papageorgiou, "Analysis and Control of a Non-Local PDE Traffic Flow Model", *International Journal of Control*, 2020, DOI: 10.1080/00207179.2020.1808902.
- [7] I. Karafyllis, D. Theodosis and M. Papageorgiou, "Two-Dimensional Cruise Control of Autonomous Vehicles on Lane-Free Roads", arXiv:2103.12205 [math.OC], 2021.
- [8] I. Karafyllis, D. Theodosis and M. Papageorgiou, "Constructing Artificial Traffic Fluids by Designing Cruise Controllers", arXiv:2203.02788, [math.OC], 2022.
- [9] R. Levy and J. Haddad, "Path and Trajectory Planning for Autonomous Vehicles on Roads without Lanes," *2021 IEEE International Intelligent Transportation Systems Conference (ITSC)*, 2021, 3871-3876.
- [10] Y. Liu, and B. Xu, "Improved Protocols and Stability Analysis for Multivehicle Cooperative Autonomous Systems", *IEEE Transactions on Intelligent Transportation Systems*, 16, 2015 2700-2710.
- [11] M. Malekzadeh, I. Papamichail, M. Papageorgiou and K. Bogenberger, "Optimal Internal Boundary Control of Lane-Free Automated Vehicle Traffic", *Transportation Research Part C*, 126, 2021, 103060.
- [12] A. K. Mulla, A. Joshi, R. Chavan, D. Chakraborty, and D. Manjunath, "A Microscopic Model for Lane-less Traffic," *IEEE Transactions on Control of Network Systems*, 6, 2019, 415-428.
- [13] M. Papageorgiou, K. -S. Mountakis, I. Karafyllis, I. Papamichail and Y. Wang, "Lane-Free Artificial-Fluid Concept for Vehicular Traffic," *Proceedings of the IEEE*, 109, 2021, 114-121.
- [14] R. Rajamani, *Vehicle Dynamics and Control*. New York, NY, USA:Springer-Verlag, 2012.
- [15] H. Tanner, A. Jadbabaie, and G. J. Pappas, "Coordination of Multiple Autonomous Vehicles", *Proceedings of IEEE Mediterranean Conference on Control and Automation*, Rhodes, Greece, 2003.
- [16] D. Troullinos, G. Chalkiadakis, I. Papamichail, and M. Papageorgiou, "Collaborative Multiagent Decision Making for Lane-Free Autonomous Driving", *AAMAS*, 2021, 1335-1343.
- [17] C. K. Verginis, D. V. Dimarogonas, "Adaptive Robot Navigation with Collision Avoidance Subject to 2nd-order Uncertain Dynamics", *Automatica*, 123, 2021, 109303.
- [18] Z. Wang, G. Wu and M. J. Barth, "A Review on Cooperative Adaptive Cruise Control (CACC) Systems: Architectures, Controls, and Applications," *2018 21st International Conference on Intelligent Transportation Systems (ITSC)*, Maui, USA, 2018, 2884-2891.
- [19] M. T. Wolf and J. W. Burdick, "Artificial Potential Functions for Highway Driving With Collision Avoidance," *2008 IEEE International Conference on Robotics and Automation*, Pasadena, CA, USA, 2008, 3731-3736.
- [20] V.K. Yanumula, P. Typaldos, D. Troullinos, M. Malekzadeh, I. Papamichail, and M. Papageorgiou, "Optimal Path Planning for Connected and Automated Vehicles in Lane-Free Traffic", *24th IEEE International Conference on Intelligent Transportation (ITSC 2021)*, Indianapolis, USA, 2021, 3545-3552.